Optimal Peak Shaving Control Using Dynamic Demand and Feed-In Limits for Grid-Connected PV Sources With Batteries

Rampelli Manojkumar, *Student Member, IEEE*, Chandan Kumar, *Senior Member, IEEE*, Sanjib Ganguly, *Senior Member, IEEE*, and João P. S. Catalão, *Senior Member, IEEE*

***Abstract*—Peak shaving of utility grid power is an important application, which benefits both grid operators and end users. In this article, an optimal rule-based peak shaving control strategy with dynamic demand and feed-in limits is proposed for grid-connected photovoltaic (PV) systems with battery energy storage systems. A method to determine demand and feed-in limits depending on the day-ahead predictions of load demand and PV power profiles is developed. Furthermore, an optimal rule-based control strategy that determines day-ahead charge/discharge schedules of battery for peak shaving of utility grid power is proposed. The rules are formulated such that the peak utility grid demand and feed-in powers are limited to the corresponding demand and feed-in limits of the day, respectively, while ensuring that the state-of-charge (SoC) of the battery at the end of the day is the same as the SoC of the start of the day. The optimal inputs required for applying the proposed rule-based control strategy are determined using a genetic algorithm for minimizing peak energy drawn from the utility grid. The proposed control algorithm is tested for various PV power and load demand profiles using MATLAB.**

***Index Terms*—Battery energy storage systems (BESSs), peak shaving, photovoltaic (PV) energy.**

Nomenclature

A. Notations

$P_{\text{grid}}, E_{\text{grid}}$	Utility grid power (kW) and energy (kWh).
P_{pv}, P_b, P_d	PV, battery and load demand powers (kW).
$P_{d-\text{lim}}, P_{\text{fil}}$	Demand and feed-in limits of the day (kW).
$t_{\text{disch}}, t_{\text{ch1}}, t_{\text{ch2}}$	Time slots of discharging mode, charging mode 1, and charging mode 2 (h).
$E_{b-\text{ch}}$	Required energy for charging battery (kWh).
$E_{\text{pv}-\text{ch}}, E_{g-\text{ch}}$	Available PV and utility grid energy to charge battery (kWh).
$E_{b-\text{disch}}$	Energy to be discharged by the battery (kWh).
$E_{b-\text{rated}}$	Rated energy capacity of battery (kWh).
C_g	Coefficient of utility grid energy to charge the battery.
$E^*_{b-\text{disch}}$	Dischargable energy of battery (kWh).
$P_{d-\text{lim0}}, P_{\text{fil0}}$	Operating demand and feed-in limits (kW).
$P_{d-\text{lim1}}, P_{d-\text{lim2}}$	Initial demand limits (kW).
$P_{\text{fil1}}, P_{\text{fil2}}$	Initial feed-in limits (kW).
$P_{b-\text{ch}}, P_{b-\text{disch}}$	Charging and discharging power of battery (kW).
$Ah_{b-\text{rated}}$	Rated ampere-hour capacity of battery (Ah).
e	Tolerance of the regula falsi method.
m	Slope in the regula falsi method.
$P_{\text{pv}-\text{ch}}, P_{g-\text{ch}}$	Available PV and utility grid powers to charge battery (kW).
$P_{d-\text{peak}}, P_{\text{pv}-\text{ins}}$	Peak load demand and installed PV power (kW).
SoC	State of charge of battery.
$\text{SoC}_i, \text{SoC}_f$	SoC at the start and end of the day.
$\text{SoC}_l, \text{SoC}_u$	Lower and upper limits of SoC.
t_0	Initial time (h).
t_1	Time when available PV power to charge the battery is more than feed-in limit (h).
i	Current flowing through battery (A).
$E_{\text{grid}-\text{peak}}$	Peak energy drawn from the utility grid (kWh).
$P_{b-\text{ch}-\text{max}}$	Maximum charging power of battery (kW).
$P_{b-\text{disch}-\text{max}}$	Maximum discharge power of battery (kW).
EP	Energy price (INR/kWh).
EC	Energy cost over a day (INR/day).
$E_{\text{grid}-d}$	Energy demand of utility grid (kWh).
$V_{\text{max}}, V_{\text{min}}$	Maximum and minimum load bus voltages (p.u.).

B. Abbreviations

RES	Renewable energy sources.
BESS	Battery energy storage systems.
PV	Photovoltaic.
SoC	State of charge.
PUGP	Peak utility grid power.
PPS	Percentage peak shaving.

Manuscript received May 21, 2020; revised September 7, 2020 and October 29, 2020; accepted December 6, 2020. This work was supported in part by the Science and Engineering Research Board (SERB) through the ASEAN–India collaborative research project entitled "Design, control and management of distributed generation in microgrid" and in part by the SERB under Research Grant ECR/2017/001564. *(Corresponding author: Chandan Kumar.)*

Rampelli Manojkumar, Chandan Kumar, and Sanjib Ganguly are with the Department of Electronics and Electrical Engineering, Indian Institute of Technology Guwahati, Guwahati 781039, India (e-mail: manoj023manoj@gmail.com; chandank@iitg.ac.in; sganguly@iitg.ac.in).

João P. S. Catalão is with the Institute for Systems and Computer Engineering, Technology and Science, Faculty of Engineering, University of Porto, 4200-465 Porto, Portugal (e-mail: catalao@fe.up.pt).

Digital Object Identifier 10.1109/JSYST.2020.3045020

I. Introduction

It IS challenging to integrate RES with the grid because of their intermittent nature [1]. BESS is a flexible solution to absorb and store excess power available with RES and deliver it as and when required [2]. The BESS is used to reduce the energy demand of the utility grid and increase the utilization of PV energy to increase the self-consumption of the system [3]–[5]. A grid-connected BESS offers several services such as energy shifting, peak shaving, power quality improvement, and spinning reserve [6]. Peak shaving is an important application, which benefits both grid operators and end users. For grid operators, peak shaving is used to maintain balance between generation and demand, resulting in improved load factor and economical operation of generation. It also provides improved system efficiency and power reliability of the grid [7]. Similarly, peak shaving is helpful in reducing consumer's electricity bills by shifting peak demand from a high-price period to a low-price period [8]. Moreover, it offers improved power quality and reliability for end users.

Various methods are used to control BESS charge/discharge schedules such as genetic algorithm, dynamic programming, rule-based algorithms, etc. [9]–[11]. The rule-based algorithms attempt to execute instructions from a starting set of data and *if–then* statement rules [12]. These algorithms are simple to implement and develop as compared to other methods. The rule-based approaches are compared with the optimization approaches in [13] and [14]. It is shown that rule-based approaches do not provide optimality even though they are simple. However, to avoid that limitation in the proposed method, the inputs required for the proposed rule-based peak shaving control are determined optimally using the genetic algorithm.

In the case of peak shaving, the maximum limit of power that is drawn from (injected into) the utility grid is known as the demand limit (feed-in limit). Flexible day-to-day management with a battery is maintaining its SoC at the end of the day, the same as the SoC of the start of the day. In [15]–[17], for peak shaving with the battery controller, a fixed demand limit is considered. However, the feed-in limit is not considered. In [18], flexible day-to-day management, along with the effective PV energy utilization, is considered for peak shaving application. However, the demand limit is fixed. In [19], the dynamic feed-in limit is considered for peak shaving, but the demand limit is not considered. In [20], peak shaving using optimal schedules of the BESS with a dynamic demand limit is considered, but the feed-in limit is not considered.

It is known that the voltage drop issues in the distribution network are due to the peak demand, and voltage rise issues are due to peak feed-in powers. Therefore, it is important to limit both peak demand and feed-in powers for a better voltage profile in the distribution network. However, in the existing literature, the peak shaving control considering both demand and feed-in limits together is not discussed while maintaining flexible day-to-day management. To avoid that limitation, both demand and feed-in powers are considered together in the proposed method while maintaining flexible day-to-day management.

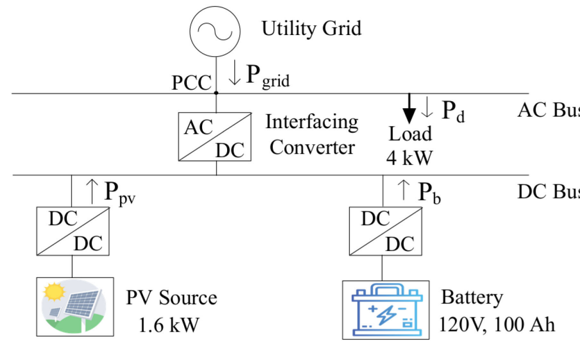

Fig. 1. Residential system with PV source, BESS, and ac load [18].

Moreover, the available PV energy and load demand over a day vary with respect to environmental conditions and seasonal changes, respectively. In this scenario, there is a possibility to limit the demand and feed-in powers to a power that is less than the fixed limit. Considering this, both demand and feed-in limits are considered as dynamic in this article. It means demand and feed-in limits are fixed over a day but vary for different days, depending on the available day-ahead predictions of load demand and PV power. These limits are given as inputs to the proposed rule-based control algorithm. The contributions of this article are as follows.

1) A method for determining the inputs required for rule-based peak shaving control, which includes both dynamic demand and feed-in limits of the day, is proposed.
2) A rule-based control algorithm that gives charge/discharge schedules of battery for peak shaving of utility grid power (limiting the utility grid demand and feed-in powers to the corresponding demand and feed-in limits of the day), considering flexible day-to-day management, is proposed.
3) The optimal inputs required for proposed rule-based peak shaving control are determined using genetic algorithm for minimizing the peak grid energy drawn from the utility grid.
4) The proposed optimal peak shaving control method is tested on the considered system. The quantitative and qualitative comparisons with the existing work are presented. Moreover, the comparison of the proposed article considering the energy cost and voltage profile of the system over a day is presented.

The rest of this article is organized as follows. Section II describes the considered system. Section III discusses the operating modes of the battery. Section IV explains the proposed method of determination of inputs. Section V discusses the proposed rule-based peak shaving control method. Section VI explains the determination of optimal inputs. Sections VII and VIII present results and conclusions, respectively.

II. System Description

A grid-connected residential end-user system consisting of PV, BESS connected at the dc bus, and ac load demand at the ac bus of the system is considered, as shown in Fig. 1 [18]. The grid is a power source that is capable of delivering/absorbing power.

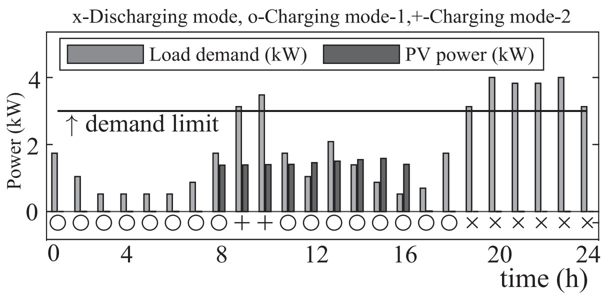

Fig. 2. Operating time slots of modes of battery (t_{disch} when $P_d(t) > P_{d-\text{lim}} \&\& P_{\text{pv}}(t) \leq P_d(t) - P_{d-\text{lim}}$; t_{ch1} when $P_d(t) \leq P_{d-\text{lim}}$; and t_{ch2} when $P_d(t) > P_{d-\text{lim}} \&\& P_{\text{pv}}(t) > P_d(t) - P_{d-\text{lim}}$).

A. Load Demand

The residential end-user load, which is considered as ac load demand, is connected at the ac bus of the system. Two types of load demand profiles, i.e., summer and winter profiles, are considered. Peak load occurs during 20:00 and 23:00 h for summer with a peak load of 4 kW, whereas it occurs during 09:00 and 12:00 h for winter with a peak load of 3.88 kW [21].

B. Interfacing Converter

The ac and dc buses are connected by a bidirectional converter known as interfacing converter (IC). The IC acts as a rectifier and an inverter, while transferring power from ac bus to dc bus and dc bus to ac bus, respectively. The IC controls the power balance and maintains constant dc-link voltage.

C. PV Source

The PV source is connected at the dc bus of the system through a dc–dc converter. This dc–dc converter helps PV source to operate at maximum power point. An installed PV power rating of 1.6 kW is considered.

D. BESS

The battery is connected to the dc bus of the system through a dc–dc converter. This dc–dc converter is used to step up the battery voltage to the dc-bus voltage. A battery with a rating of 120 V, 100 Ah is chosen for peak shaving application.

The system parameters are chosen as per [18]. The power balance equation at the point of common coupling (PCC), neglecting losses, is given as

$$P_{\text{grid}}(t) + P_{\text{pv}}(t) + P_b(t) = P_d(t). \tag{1}$$

A discrete-time model is assumed. In (1), "t" represents the time interval $[(t-1) \times T_c, t \times T_c]$, where T_c is each time slot duration, i.e., $T_c = 1$ h.

III. Operating Modes of Battery

With the considered battery along with the PV source, it is possible to limit $P_{\text{grid}}(t)$ to $P_{d-\text{lim}}$. The operating time slots of modes of battery for typical load demand and PV power profiles are indicated in Fig. 2. There are three operating modes to limit $P_{\text{grid}}(t)$ to $P_{d-\text{lim}}$ using a battery in the presence of a PV source. These are defined as follows.

1) *Discharging mode:* The discharging mode is during the time t_{disch}, when load demand is more than the demand limit and the PV source is unable to supply the required power, i.e., $P_d(t) > P_{d-\text{lim}} \&\& P_{\text{pv}}(t) \leq P_d(t) - P_{d-\text{lim}}$. The symbol "&&" indicates logical AND operator.
2) *Charging mode 1:* Charging mode 1 is during the time t_{ch1}, when load demand is less than the demand limit, i.e., $P_d(t) \leq P_{d-\text{lim}}$.
3) *Charging mode 2:* Charging mode 2 is during the time t_{ch2}, when load demand is more than the demand limit and the PV source is able to supply the required power, i.e., $P_d(t) > P_{d-\text{lim}} \&\& P_{\text{pv}}(t) > P_d(t) - P_{d-\text{lim}}$.

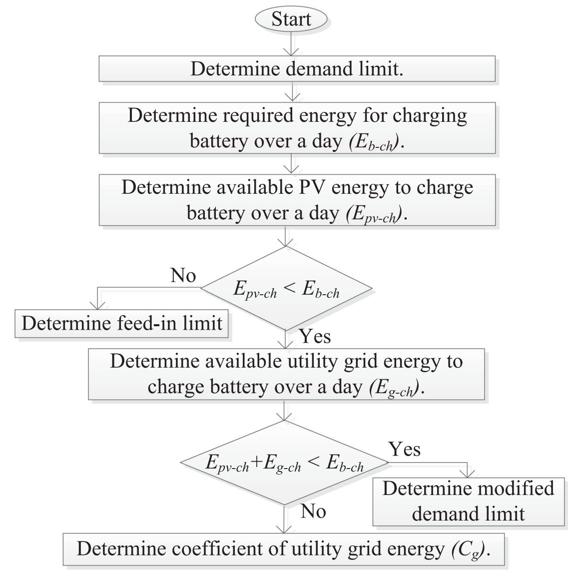

Fig. 3. Coordination of inputs required for rule-based peak shaving control algorithm.

IV. Proposed Method of Determination of Inputs

The required inputs for the proposed rule-based peak shaving control are determined using predicted load demand and PV powers. The inputs are $P_{d-\text{lim}}$, $E_{b-\text{ch}}$, $E_{\text{pv}-\text{ch}}$, $E_{g-\text{ch}}$, C_g, $P^m_{d-\text{lim}}$, and P_{fil}. The coordination of these inputs is given in the flowchart in Fig. 3. First, $P_{d-\text{lim}}$, $E_{b-\text{ch}}$, and $E_{\text{pv}-\text{ch}}$ are determined. Then, $E_{g-\text{ch}}$ is determined if $E_{\text{pv}-\text{ch}} \leq E_{b-\text{ch}}$. The $P^m_{d-\text{lim}}$ is determined if $E_{\text{pv}-\text{ch}} + E_{g-\text{ch}} \leq E_{b-\text{ch}}$; otherwise, C_g is determined. P_{fil} is determined if $E_{\text{pv}-\text{ch}} > E_{b-\text{ch}}$. These inputs are used for determining battery charge/discharge schedules for peak shaving control. The method of determination of these inputs is discussed as follows.

A. Demand Limit

Let us define a control variable known as the dischargeable energy of battery over a day ($E^*_{b-\text{disch}}$) which is chosen between 0 kWh and $E_{b-\text{rated}}$ (including both 0 kWh and $E_{b-\text{rated}}$), i.e.,

$$0 \leq E^*_{b-\text{disch}} \leq E_{b-\text{rated}}. \tag{2}$$

Since $E_{b-\text{rated}}$ is 12 kWh, $E^*_{b-\text{disch}} \in [0, 12]$ kWh.

The demand limit is determined such that $E_{b-\text{disch}}$ is equal to $E^*_{b-\text{disch}}$. Therefore, we have

$$E_{b-\text{disch}} = E^*_{b-\text{disch}} \tag{3}$$

$$\sum P_{b-\text{disch}}(t) - E^*_{b-\text{disch}} = 0 \quad \forall t \in t_{\text{disch}}. \tag{4}$$

To limit $P_{\text{grid}}(t)$ to $P_{d-\text{lim}}$, the required amount of power $P_d(t) - P_{d-\text{lim}}$ is supplied either by PV source or battery to load when $P_d(t) > P_{d-\text{lim}}$. However, the battery provides the amount of power that could not be supplied by the PV source. Therefore, we have

$$\begin{aligned} P_{b-\text{disch}}(t) &= (P_d(t) - P_{d-\text{lim}}) - P_{\text{pv}}(t) \quad \forall t \in t_{\text{disch}} \\ &= 0, \text{ otherwise.} \end{aligned} \tag{5}$$

Substituting (5) into (4) gives

$$\sum((P_d(t) - P_{d-\text{lim}}) - P_{\text{pv}}(t)) - E^*_{b-\text{disch}} = 0 \quad \forall t \in t_{\text{disch}}. \tag{6}$$

Equation (6) is in form of $f(P_{d-\text{lim}}) = 0$, where

$$f(P_{d-\text{lim}}) = \sum((P_d(t) - P_{d-\text{lim}}) - P_{\text{pv}}(t)) - E^*_{b-\text{disch}} \quad \forall t \in t_{\text{disch}}. \tag{7}$$

In (7), $P_{d-\text{lim}}$ is an independent variable. To solve for $P_{d-\text{lim}}$, the root-finding algorithm of the regula falsi method is used [22]. The regula falsi method is a combination of the secant method and the bisection search theorem. The regula falsi method is faster than the bisection method, and root convergence is guaranteed. According to the regula falsi method, $(P_{d-\text{lim1}}, P_{d-\text{lim2}})$ are chosen such that $f(P_{d-\text{lim1}})$ is positive and $f(P_{d-\text{lim2}})$ is negative. Then, $P_{d-\text{lim0}}$ is determined as follows:

$$\begin{aligned} P_{d-\text{lim0}} &= \frac{1}{m}(0 - f(P_{d-\text{lim1}})) + P_{d-\text{lim1}}, \text{ where} \\ m &= \frac{f(P_{d-\text{lim2}}) - f(P_{d-\text{lim1}})}{(P_{d-\text{lim2}} - P_{d-\text{lim1}})}. \end{aligned} \tag{8}$$

Using (24), we determine $f(P_{d-\text{lim0}})$. When $|f(P_{d-\text{lim0}})| < e$, $P_{d-\text{lim0}}$ becomes $P_{d-\text{lim}}$. When $|f(P_{d-\text{lim0}}| > e$, either replace $P_{d-\text{lim1}}$ by $P_{d-\text{lim0}}$ (if $f(P_{d-\text{lim0}}) > 0$) or replace $P_{d-\text{lim2}}$ by $P_{d-\text{lim0}}$ (if $f(P_{d-\text{lim0}}) < 0$). Then, continue the above process till $P_{d-\text{lim0}}$ becomes $P_{d-\text{lim}}$. The applied regula falsi method to determine $P_{d-\text{lim}}$ is shown as a flowchart in Fig. 4.

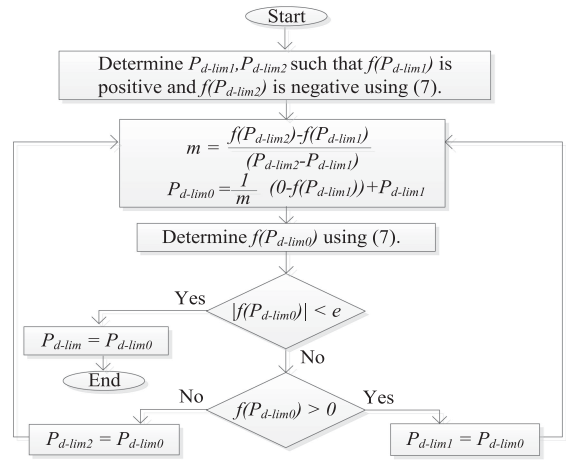

Fig. 4. Determination of demand limit using the regula falsi method.

B. Required Energy for Charging Battery Over a Day

For flexibility of day-to-day management, the required energy for charging battery over a day must be equal to the energy to be discharged from battery over a day, i.e.,

$$E_{b-\text{ch}} = E_{b-\text{disch}} = E^*_{b-\text{disch}}. \tag{9}$$

C. Available PV Energy to Charge the Battery Over a Day

From (9), the battery is to be charged by the amount of energy $E_{b-\text{ch}}$, either by the PV source or the utility grid. First, the available PV energy to charge the battery over a day (without injecting into grid) is calculated. If it is not sufficient, then the available utility grid energy to charge the battery is determined. The $P_{\text{pv}-\text{ch}}$ is $P_{\text{pv}}(t)$ and $P_{\text{pv}}(t) - (P_d(t) - P_{d-\text{lim}})$ during t_{ch1} and t_{ch2}, respectively, i.e.,

$$\begin{aligned} P_{\text{pv}-\text{ch}} &= P_{\text{pv}}(t) \quad \forall t \in t_{\text{ch1}} \\ &= P_{\text{pv}}(t) - (P_d(t) - P_{d-\text{lim}}) \quad \forall t \in t_{\text{ch2}} \\ &= 0, \text{ otherwise.} \end{aligned} \tag{10}$$

Then, the available PV energy for charging battery over a day is the sum of $P_{\text{pv}-\text{ch}}(t)$ over a day as given in

$$E_{\text{pv}-\text{ch}} = \sum_{t=1}^{T} P_{\text{pv}-\text{ch}}(t) \tag{11}$$

where T is the predictive horizon of 24 h.

D. Available Utility Grid Energy to Charge the Battery Over a Day

From (9) and (11), if $E_{\text{pv}-\text{ch}} \leq E_{b-\text{ch}}$, it means that the available PV energy is not sufficient to charge the battery with the required amount of energy. Then, deficit amount of energy is drawn from the utility grid provided that its demand is not more than the demand limit. It means that the utility grid is not used to charge the battery during t_{ch2}. Then, during t_{ch1}, the available power from the utility grid to charge the battery ($P_{g-\text{ch}}(t)$) for limiting P_{grid} to $P_{d-\text{lim}}$ is $P_{d-\text{lim}} - P_d(t)$, i.e.,

$$\begin{aligned} P_{g-\text{ch}}(t) &= P_{d-\text{lim}} - P_d(t) \quad \forall t \in t_{\text{ch1}} \\ &= 0, \text{ otherwise.} \end{aligned} \tag{12}$$

Then, the available utility grid energy for charging battery over a day is the sum of $P_{g-\text{ch}}(t)$ over a day as given in

$$E_{g-\text{ch}} = \sum_{t=1}^{T} P_{g-\text{ch}}(t). \tag{13}$$

E. Coefficient of Utility Grid Energy to Charge the Battery

From (9), (11), and (13), if $E_{\text{pv}-\text{ch}} \leq E_{b-\text{ch}} \&\& E_{g-\text{ch}} + E_{\text{pv}-\text{ch}} > E_{b-\text{ch}}$, the deficit amount of energy for completely charging battery, i.e., $E_{b-\text{ch}} - E_{\text{pv-ch}}$, has to be supplied by the utility grid. However, only a fraction of utility grid energy is required to charge the battery while utilizing the total available PV energy for charging battery. In this case, if $C_g E_{g-\text{ch}}$ is considered as the required utility grid energy to charge the battery, it is equal to $E_{b-\text{ch}} - E_{\text{pv-ch}}$, as

$$C_g E_{g-\text{ch}} = E_{b-\text{ch}} - E_{\text{pv-ch}}$$
$$C_g = \frac{E_{b-\text{ch}} - E_{\text{pv-ch}}}{E_{g-\text{ch}}}. \tag{14}$$

F. Modified Demand Limit

From (9), (11), and (13), if $E_{g-\text{ch}} + E_{\text{pv-ch}} \leq E_{b-\text{ch}}$, it means that the battery is unable to charge with the required amount of energy to limit $P_{\text{grid}}(t)$ to $P_{d-\text{lim}}$. In this case, SoC_f cannot be equal to SoC_i, which results in violation of flexible day-to-day management. To avoid this violation, $P_{d-\text{lim}}$ is modified such that the sum of the available energy from the utility grid and the PV source to charge the battery over T is equal to the energy to be discharged by the battery over T, i.e.,

$$\sum_{t=1}^{T} P^m_{g-\text{ch}}(t) + \sum_{t=1}^{T} P^m_{\text{pv-ch}}(t) = \sum_{t=1}^{T} P^m_{b-\text{disch}}(t). \tag{15}$$

Superscript "m" indicates respective quantities for modified demand limit $P^m_{d-\text{lim}}$. Using (5), (10), and (12), substituting $P^m_{b-\text{disch}}(t)$, $P^m_{\text{pv-ch}}(t)$, and $P^m_{g-\text{ch}}(t)$ into (15) for t^m_{ch1}, t^m_{ch2}, and t^m_{disch} gives

$$\sum (P^m_{d-\text{lim}} - P_d(t)) + (P_{\text{pv}}(t)) - (0) = 0 \quad \forall t \in t^m_{\text{ch1}} \tag{16}$$

$$\sum (0) + (P_{\text{pv}}(t) - (P_d(t) - P^m_{d-\text{lim}})) - (0) = 0 \quad \forall t \in t^m_{\text{ch2}} \tag{17}$$

$$\sum (0) + (0) - (-(P_{\text{pv}}(t) - (P_d(t) - P^m_{d-\text{lim}}))) = 0$$
$$\forall t \in t^m_{\text{disch}}. \tag{18}$$

Combining (16)–(18) over T gives

$$\sum_{t=1}^{T} (P_{\text{pv}}(t) - (P_d(t) - P^m_{d-\text{lim}})) = 0. \tag{19}$$

Then, the modified demand limit is given as

$$P^m_{d-\text{lim}} = \frac{\sum_{t=1}^{T} (P_d(t) - P_{\text{pv}}(t))}{T}. \tag{20}$$

G. Feed-in Limit

From (9) and (11), if $E_{\text{pv-ch}} > E_{b-\text{ch}}$, then complete available PV energy is not required to charge the battery with the required amount of energy. Therefore, a limit of PV power P_{fil} is determined such that the PV source is not used to charge the battery when $P_{\text{pv-ch}}(t) \leq P_{\text{fil}}$ and is completely charged with $P_{\text{pv-ch}}(t) - P_{\text{fil}}$ when $P_{\text{pv-ch}}(t) > P_{\text{fil}}$ during t_{ch}, i.e.,

$$\sum (P_{\text{pv-ch}}(t) - P_{\text{fil}}) = E_{b-\text{ch}} \quad \forall t \in t_{\text{ch}} \&\& t_1. \tag{21}$$

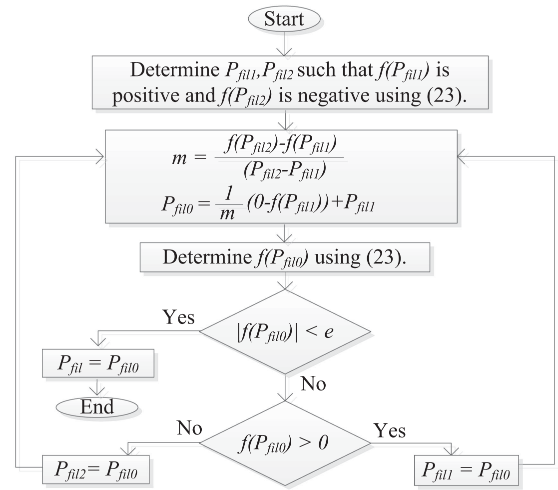

Fig. 5. Determination of feed-in limit using the regula falsi method.

In (21), t_1 is the time when $P_{\text{pv-ch}}(t) > P_{\text{fil}}$. Moreover, $P_{\text{pv-ch}}(t) = P_{\text{pv}}(t)$ when $t_{\text{ch}} = t_{\text{ch1}}$ and $P_{\text{pv-ch}}(t) = P_{\text{pv}}(t) - (P_d(t) - P_{d-\text{lim}})$ when $t_{\text{ch}} = t_{\text{ch2}}$

$$\sum (P_{\text{pv-ch}}(t) - P_{\text{fil}}) - E_{b-\text{ch}} = 0 \quad \forall t \in t_{\text{ch}} \&\& t_1. \tag{22}$$

Equation (22) is in form of $f(P_{\text{fil}}) = 0$, where

$$f(P_{\text{fil}}) = \sum (P_{\text{pv-ch}}(t) - P_{\text{fil}}) - E_{b-\text{ch}} \qquad \forall t \in t_{\text{ch}} \&\& t_1. \tag{23}$$

In (22), P_{fil} is an independent variable. Therefore, to solve for P_{fil}, the root finding algorithm of the regula falsi method is used. The determination of P_{fil} using the regula falsi method is similar to the determination of $P_{d-\text{lim}}$. First, $(P_{\text{fil1}}, P_{\text{fil2}})$ are chosen such that $f(P_{\text{fil1}})$ is positive and $f(P_{\text{fil2}})$ is negative. Then, P_{fil0} is determined as follows:

$$P_{\text{fil0}} = \frac{1}{m}(0 - f(P_{\text{fil1}})) + P_{\text{fil1}}, \text{ where}$$
$$m = \frac{f(P_{\text{fil2}}) - f(P_{\text{fil1}})}{(P_{\text{fil2}} - P_{\text{fil1}})}. \tag{24}$$

Using (24), we determine $f(P_{\text{fil0}})$. When $|f(P_{\text{fil0}})| < e$, P_{fil0} becomes P_{fil}. When $|f(P_{\text{fil0}}| > e$, either replace P_{fil1} by P_{fil0} (if $f(P_{\text{fil0}}) > 0$) or replace P_{fil2} by P_{fil0} (if $f(P_{\text{fil0}}) < 0$). Then, continue the above process till P_{fil0} becomes P_{fil}. The applied regula falsi method to determine P_{fil} is shown as a flowchart in Fig. 5.

V. Proposed Rule-Based Peak Shaving Control

Considering the above determined inputs, rules for peak shaving control are formulated to know the day-ahead charge/discharge schedules of battery. These rules are formulated such that the day-to-day management is flexible while limiting peak utility grid demand and feed-in powers to the corresponding demand and feed-in limits, respectively. The formulated rules during discharging and charging modes are explained in this section.

TABLE I
UTILITY GRID POWER

Mode of operation	Rule	Utility grid power
Discharging mode	1	P_{d-lim}
Charging mode-1	2	$P_d(t) + C_g(P_{d-lim} - P_d(t))$
Charging mode-1	3	P_{d-lim}^m
Charging mode-1	4	$P_d(t) - P_{fil}$
Charging mode-1	5	$P_d(t) - P_{pv}(t)$
Charging mode-2	6	P_{d-lim}
Charging mode-2	7	$P_{d-lim} - P_{fil}$
Charging mode-2	8	$P_d(t) - P_{pv}(t)$

A. *Discharging Mode (During t_{disch})*

Rule 1: The battery discharges by the amount $(P_d(t) - P_{d-\text{lim}}) - P_{\text{pv}}(t)$ as per (5).

B. *Charging Mode 1 (During t_{ch1})*

Rule 2: If $E_{\text{pv}-\text{ch}} \leq E_{b-\text{ch}} \&\& E_{\text{pv}-\text{ch}} + E_{g-\text{ch}} > E_{b-\text{ch}}$, the PV source and the utility grid are used to charge the battery by the amount $P_{\text{pv}}(t) + C_g(P_{d-\text{lim}} - P_d(t))$ as per (10), (12), and (14).

Rule 3: If $E_{\text{pv}-\text{ch}} \leq E_{b-\text{ch}} \&\& E_{\text{pv}-\text{ch}} + E_{g-\text{ch}} \leq E_{b-\text{ch}}$, the PV source and the utility grid are used to charge the battery by the amount $P_{\text{pv}}(t) + (P_{d-\text{lim}}^m - P_d(t))$ as per (16).

Rule 4: If $E_{\text{pv}-\text{ch}} > E_{b-\text{ch}} \&\& P_{\text{pv}}(t) > P_{\text{fil}}$, the PV source is used to charge the battery by the amount $P_{\text{pv}}(t) - P_{\text{fil}}$ as per (10) and (21).

Rule 5: If $E_{\text{pv}-\text{ch}} > E_{b-\text{ch}} \&\& P_{\text{pv}}(t) \leq P_{\text{fil}}$, the PV source is not used to charge the battery.

C. *Charging Mode 2 (During t_{ch2})*

Rule 6: If $E_{\text{pv}-\text{ch}} \leq E_{b-\text{ch}}$, the PV source is used to charge the battery by the amount $P_{\text{pv}}(t) - (P_d(t) - P_{d-\text{lim}})$ as per (10).

Rule 7: If $E_{\text{pv}-\text{ch}} > E_{b-\text{ch}} \&\& (P_{\text{pv}}(t) - (P_d(t) - P_{d-\text{lim}})) > P_{\text{fil}}$, the PV source is used to charge the battery by the amount $(P_{\text{pv}}(t) - (P_d(t) - P_{d-\text{lim}})) - P_{\text{fil}}$ as per (10) and (21).

Rule 8: If $E_{\text{pv}-\text{ch}} > E_{b-\text{ch}} \&\& (P_{\text{pv}}(t) - (P_d(t) - P_{d-\text{lim}})) \leq P_{\text{fil}}$, the PV source is not used to charge the battery.

The SoC of the battery during discharging and charging modes is calculated using the coulomb-counting method [23] as follows:

$$\text{SoC}(t) = 1 - \frac{\sum_{t_0}^{t} i}{Ah_{b-\text{rated}}} \tag{25}$$

where the current i is positive for discharging and negative for charging.

Considering the aforementioned Rules 1–8 and (1), the resulting utility grid power is given in Table I.

TABLE II
SYSTEM PARAMETERS [18]

Parameter	Value	Parameter	Value
P_{d-peak}	4 kW	SoC_l/SoC_u	0.2/0.9
P_{pv-ins}	1.6 kW	SoC_i	0.5
$E_{b-rated}$	12 kWh	$P_{b-ch-max}$	3 kW
$Ah_{b-rated}$	100 Ah	$P_{b-disch-max}$	3 kW

VI. DETERMINATION OF OPTIMAL INPUTS

Peak shaving of utility grid power with the optimal utilization of battery is important. The optimal problem formulation is discussed as follows.

The considered fitness function and constraints are given as follows:

$$\text{minimize } f = E_{\text{grid}-\text{peak}} \tag{26}$$

subjected to

$$P_{\text{grid}}(t) + P_{\text{pv}}(t) + P_b(t) = P_d(t) \tag{27}$$

$$\text{SoC}_l \leq \text{SoC}(t) \leq \text{SoC}_u, \text{SoC}_f = \text{SoC}_i \tag{28}$$

$$P_{b-\text{ch}}(t) \leq P_{b-\text{ch}-\text{max}}, P_{b-\text{disch}}(t) \leq P_{b-\text{disch}-\text{max}} \tag{29}$$

$$E_{b-\text{disch}}^* \leq E_{b-\text{rated}}. \tag{30}$$

Equation (26) says that the objective is to minimize $E_{\text{grid}-\text{peak}}$. Equation (27) indicates the power balance constraint. Equation (28) indicates the constraints of SoC limits of the battery and the flexible day-to-day operation of the battery. Equations (29) and (30) indicate the constraints of charge/discharge powers of the battery and dischargeable energy of the battery over a day, respectively. The system parameters along with the constraints are shown in Table II [18].

In (26), $E_{\text{grid}-\text{peak}}$ is the peak energy drawn from the utility grid over the day, i.e.,

$$E_{\text{grid}-\text{peak}} = \text{maximum}(E_{\text{grid}}(t)) \quad \forall t \in [0, T]. \tag{31}$$

E_{grid} is determined as

$$E_{\text{grid}}(t) = (P_{\text{grid}}(t)) \times T_c. \tag{32}$$

$E_{b-\text{disch}}^*$ is considered as control variable, since the required inputs for peak shaving control depend on $E_{b-\text{disch}}^*$, as discussed earlier. The formulated problem is an offline optimization problem with a nonlinear fitness function, which is solved using the genetic algorithm (GA) solver in MATLAB. The genetic algorithm is a popular heuristic optimization technique for solving a nonlinear optimization problem [24]. A population size of 20 is considered.

The method of determination of optimal dischargeable energy of the battery ($E_{ob-\text{disch}}^*$) using the ga solver is shown as a flowchart in Fig. 6. Once $E_{ob-\text{disch}}^*$ is determined, the inputs corresponding to $E_{ob-\text{disch}}^*$ are considered as the optimal inputs required for the proposed rule-based control, i.e., $P_{od-\text{lim}}$, $E_{ob-\text{ch}}$, $E_{\text{opv}-\text{ch}}$, $E_{og-\text{ch}}$, C_{og}, $P_{od-\text{lim}}^m$, and P_{ofil}. It means the output of optimization, i.e., solving of the optimization problem, gives the optimal rule-based inputs. Later, these optimal rule-based

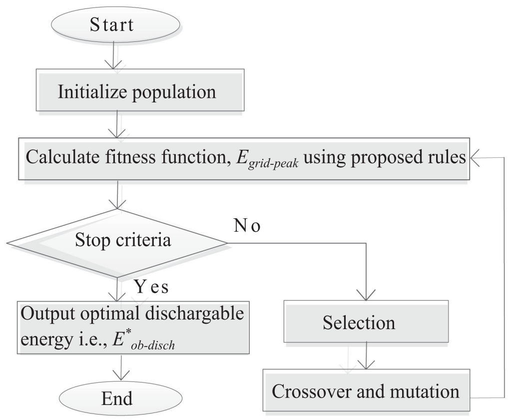

Fig. 6. Genetic algorithm for determining optimal dischargeable energy of the battery.

TABLE III
OPTIMAL INPUTS OF CONTROL ALGORITHM FOR FOUR CASES

Input Parameter	Case 1	Case 2	Case 3	Case 4
P_{od-lim} (kW)	1.72	2.437	2.853	2.852
E_{ob-ch} (kWh)	5.4615	6.5353	4.7937	5.4804
E_{opv-ch} (kWh)	5.6933	0.0202	12.1922	0.0668
E_{og-ch} (kWh)	NA	20.668	NA	28.0673
C_{og}	NA	0.3152	NA	0.1929
P^m_{od-lim} (kW)	NA	NA	NA	NA
P_{ofil} (kW)	0.0543	NA	0.8249	NA

inputs are used to determine optimal battery schedules using the proposed rule-based peak shaving control algorithm. The proposed peak shaving control is shown as a flowchart in Fig. 7.

VII. RESULTS

The proposed method is tested on the considered system for various load and PV power profiles to show the applicability for any grid-connected PV system with the BESS. The optimal inputs required for applying the control algorithm for these cases are determined and given in Table III. The plot of best fitness value and generations for multiple runs of genetic algorithm for the case of winter load profile with more PV availability is shown in Fig. 8. The minimum value among these best fitness values (considering all runs), i.e., 1.72 kWh, is the optimal peak energy drawn from the utility grid. The obtained results with proposed method are discussed for these cases as follows.

Case 1: Winter Load Profile With More PV Energy Availability

In this case, the load demand profile of winter with more PV energy availability over a day is considered, as shown in Fig. 9(a). The determined $P_{od-\text{lim}}$, $E_{ob-\text{ch}}$, $E_{\text{opv}-\text{ch}}$, and P_{ofil} are 1.72 kW, 5.4615 kWh, 5.6933 kWh, and 0.0543 kW, respectively. The available PV energy to charge the battery is more than the required energy for charging the battery ($E_{\text{opv}-\text{ch}} > E_{ob-\text{ch}}$). Therefore, $E_{og-\text{ch}}$, C_{og}, and $P^m_{od-\text{lim}}$ are not applicable (NA) in this case, as given in Table III. As per Fig. 2 for the determined $P_{od-\text{lim}}$, the discharging mode is during t = 4, 5, 6, 7, 8, 9, 10, 11, 12, 19, 20, 21, and 22 h, charging mode 1 is during t = 1, 2, 3, 14, 15, 16, 17, 18, 23, and 24 h, and charging mode 2 is during $t = 13$ h. Resulting optimal charge/discharge schedules of the battery for these modes are shown in Fig. 9(b). It is observed that the battery is charged only by the PV source. The SoC for these battery schedules is shown in Fig. 9(c). Fig. 9(c) shows that $\text{SoC}_f = \text{SoC}_i = 50\%$, which is desired for flexible day-to-day management. The resulting utility grid demand is shown in Fig. 9(d). This indicates that the utility grid demand is limited to $P_{od-\text{lim}}$ of 1.72 kW, and there is no feed-in power into the grid.

Case 2: Winter Load Profile With Less PV Energy Availability

In this case, the load demand profile of winter with less PV energy availability over a day is considered, as shown in Fig. 10(a). The determined $P_{od-\text{lim}}$, $E_{ob-\text{ch}}$, $E_{\text{opv}-\text{ch}}$, $E_{og-\text{ch}}$, and C_{og} are 2.437 kW, 6.5353 kWh, 0.0202 kWh, 20.668 kWh, and 0.3152, respectively. The available PV energy to charge the battery is less than the required energy for charging the battery. Moreover, the sum of the available PV and utility grid energy is more than the required energy for charging the battery ($E_{\text{pv}-\text{ch}} \le E_{b-\text{ch}} \&\& E_{g-\text{ch}} + E_{\text{pv}-\text{ch}} > E_{b-\text{ch}}$). Therefore, $P^m_{od-\text{lim}}$ and P_{ofil} are not applicable (NA) in this case, as given in Table III. As per Fig. 2 for the determined $P_{od-\text{lim}}$, the discharging mode is during t = 7, 8, 9, 10, 11, 12, and 21 h, and charging mode 1 is during t = 1, 2, 3, 4, 5, 6, 13, 14, 15, 16, 17, 18, 19, 20, 22, 23, and 24 h. There is no charging mode 2 in this case due to less availability of PV power over a day. Resulting optimal charge/discharge schedules of the battery for these modes are shown in Fig. 10(b). It is observed that the battery is charged by both the PV source and the utility grid. The SoC for these battery schedules is shown in Fig. 10(c). Fig. 10(c) shows that $\text{SoC}_f = \text{SoC}_i = 50\%$, which is desired for flexible day-to-day management. The resulting utility grid demand is shown in Fig. 10(d). This indicates that the utility grid demand is limited to $P_{od-\text{lim}}$ of 2.437 kW, and there is no feed-in power into the grid.

Case 3: Summer Load Profile With More PV Energy Availability

In this case, the load demand profile of summer with more PV energy availability over a day is considered, as shown in Fig. 11(a). The determined $P_{od-\text{lim}}$, $E_{ob-\text{ch}}$, $E_{\text{opv}-\text{ch}}$, and P_{ofil} are 2.853 kW, 4.7937 kWh, 12.1922 kWh, and 0.8279 kW, respectively. The available PV energy to charge the battery is more than the required energy for charging the battery ($E_{\text{opv}-\text{ch}} > E_{ob-\text{ch}}$). Therefore, the $E_{og-\text{ch}}$, C_{og}, and $P^m_{od-\text{lim}}$ are not applicable (NA) in this case, as given in Table III. As per Fig. 2 for the determined $P_{od-\text{lim}}$, the discharging mode is during t = 19, 20, 21, 22, 23, and 24 h, charging mode 1 is during t = 1, 2, 3, 4, 5, 6, 7, 8, 11, 12, 13, 14, 15, 16, 17, and 18 h, and charging mode 2 is during t = 9 and 10 h. Resulting optimal charge/discharge schedules of the battery for these modes are shown in Fig. 11(b). It is observed that only the PV source is used to charge the battery. The SoC for these battery schedules is shown in Fig. 11(c). Fig. 11(c) shows that $\text{SoC}_f = \text{SoC}_i = 50\%$, which is desired for flexible day-to-day management. The resulting utility grid demand is

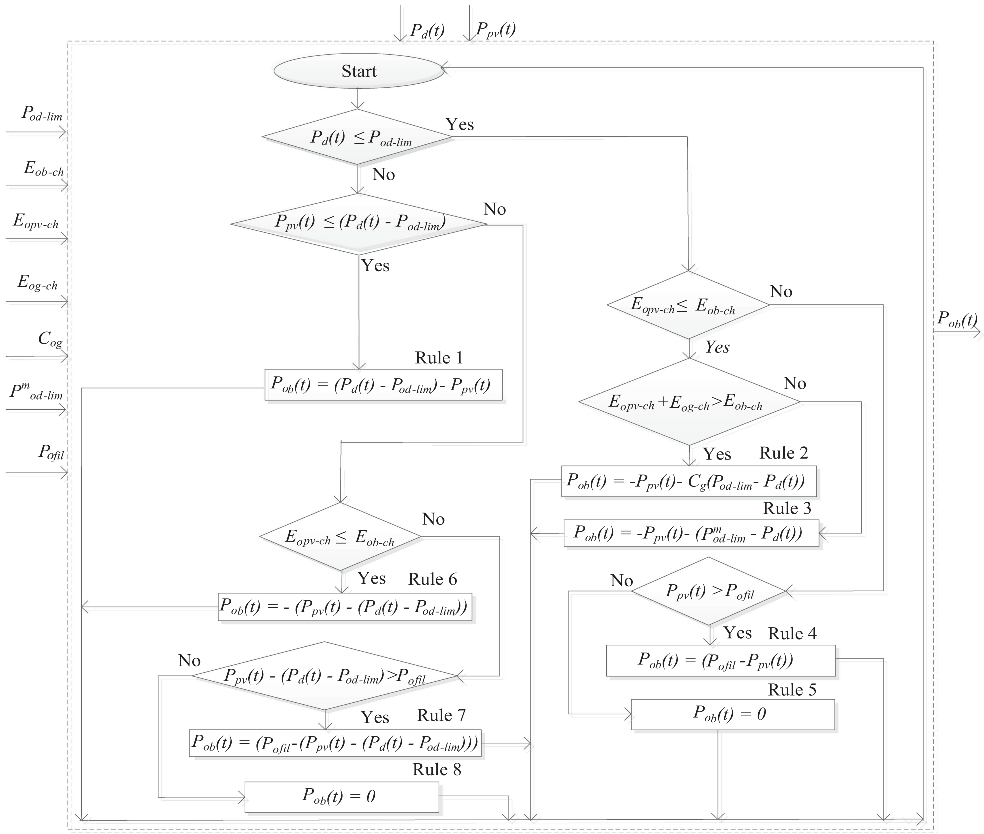

Fig. 7. Proposed optimal rule-based peak shaving control algorithm.

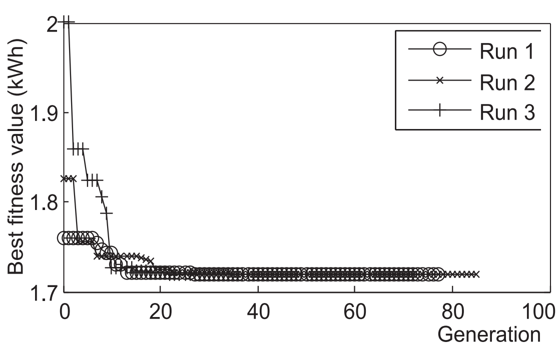

Fig. 8. Case 1: Best fitness values for multiple simulation runs.

shown in Fig. 11(d). This indicates that the utility grid demand is limited to $P_{od-\lim}$ of 2.853 kW, and the feed-in power is limited to $P_{\rm ofil}$ of 0.8249 kW.

Case 4: Summer Load Profile With Less PV Energy Availability

In this case, the load demand profile of summer with less PV energy availability is considered, as shown in Fig. 12(a). The determined $P_{od-\lim}$, $E_{ob-{\rm ch}}$, $E_{opv-{\rm ch}}$, $E_{og-{\rm ch}}$, and C_{og} are 2.852 kW, 5.4804 kWh, 0.0668 kWh, 28.0673 kWh, and 0.1929, respectively. The available PV energy to charge the

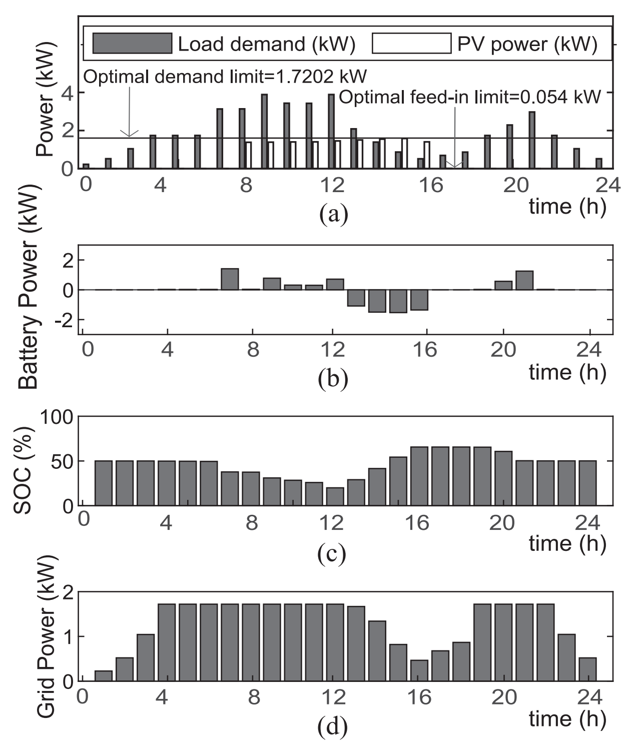

Fig. 9. Case 1. (a) Load demand and PV power profiles. (b) Charge/discharge schedules of the battery. (c) SoC of the battery. (d) Utility grid power.

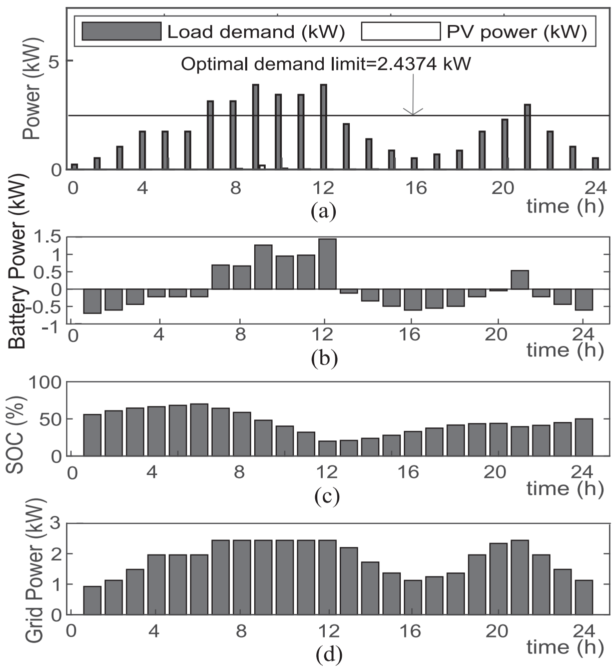

Fig. 10. Case 2. (a) Load demand and PV power profiles. (b) Charge/discharge schedules of the battery. (c) SoC of the battery. (d) Utility grid power.

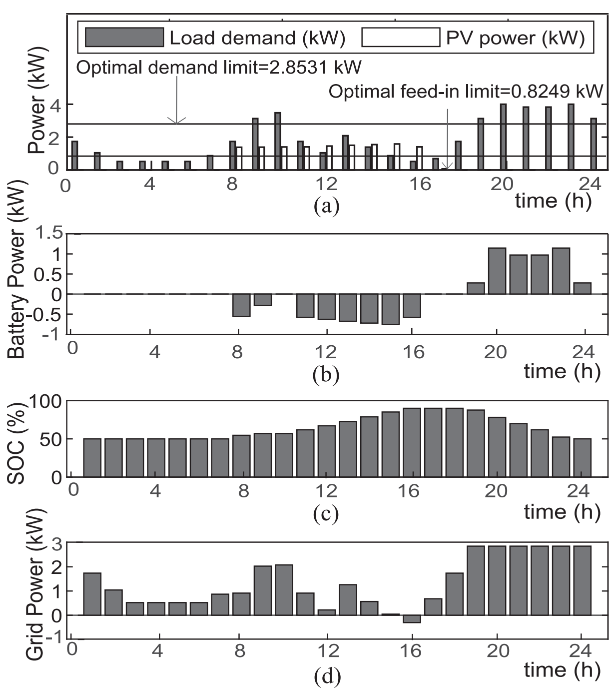

Fig. 11. Case 3. (a) Load demand and PV power profiles. (b) Charge/discharge schedules of the battery. (c) SoC of the battery. (d) Utility grid power.

battery is less than the required energy for charging the battery. Moreover, the sum of the available PV and utility grid energy is more than the required energy for charging the battery ($E_{\text{pv}-\text{ch}} \leq E_{b-\text{ch}} \&\& E_{g-\text{ch}} + E_{\text{pv}-\text{ch}} > E_{b-\text{ch}}$). Therefore, $P^m_{od-\text{lim}}$ and P_{ofil} are not applicable in this case, as given in Table III. As per Fig. 2 for the determined $P_{od-\text{lim}}$, the discharging mode is during $t = 9$, 10, 19, 20, 21, 22, 23, and 24 h, and

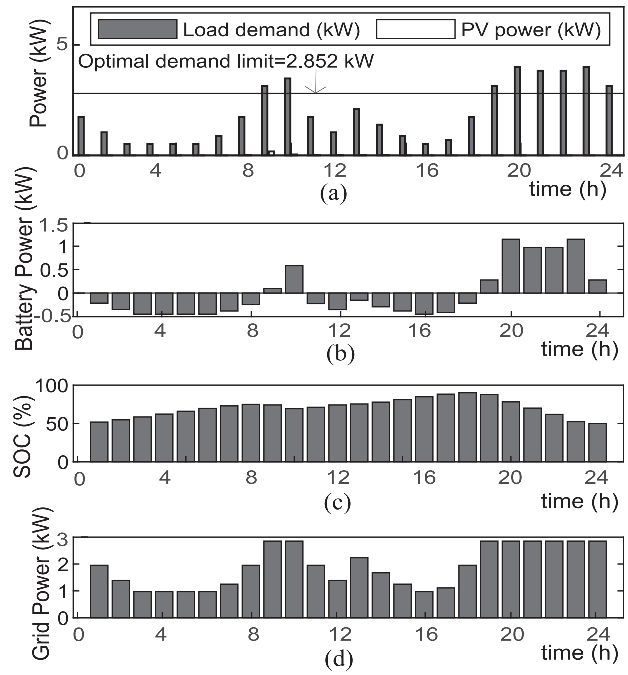

Fig. 12. Case 4. (a) Load demand and PV power profiles. (b) Charge/discharge schedules of the battery. (c) SoC of the battery. (d) Utility grid power.

TABLE IV
QUANTITATIVE COMPARISON OF THE PROPOSED WORK WITH THE EXISTING WORK

Parameter	Ref. [18]	Proposed			
		Case 1	Case 2	Case 3	Case 4
PUGP(kW)	3	1.72	2.437	2.853	2.852
PPS(%)	25	55.66	37.18	28.67	28.7

charging mode 1 is during $t = 1$, 2, 3, 4, 5, 6, 7, 8, 11, 12, 13, 14, 15, 16, 17, and 18 h. There is no charging mode 2 in this case due to less availability of PV energy. Resulting optimal charge/discharge schedules of the battery for these modes are shown in Fig. 12(b). It is observed that both the PV source and the utility grid are used to charge the battery. The SoC for these battery schedules is shown in Fig. 12(c). Fig. 12(c) shows that $\text{SoC}_f = \text{SoC}_i = 50\%$, which is desired for flexible day-to-day management. The resulting utility grid demand is shown in Fig. 12(d). This indicates that the utility grid demand is limited to $P_{od-\text{lim}}$ of 2.852 kW, and there is no feed-in power into the grid.

A. Comparative Analysis

The comparative analysis of the proposed method is discussed as follows.

1) Quantitative Comparison: The system and its ratings chosen in the proposed article are the same as those of the system chosen in [18]. Therefore, the proposed article is quantitatively compared with [18]. The quantitative comparison considering PUGP and PPS is shown in Table IV. The table indicates that PUGP is limited to a fixed value of 3 kW in [18]. In the proposed method, PUGP is limited to 1.72 kW, 2.437 kW, 2.853 kW,

TABLE V
ENERGY COST AND MAXIMUM AND MINIMUM BUS VOLTAGES IN FOUR CASES

Parameter	Case 1		Case 2		Case 3		Case 4	
	without BESS	Proposed	without BESS	Proposed	without BESS	Proposed	without BESS	Proposed
EC (INR/day)	162.3459	149.5737	217.2627	209.7624	179.2068	166.5379	228.1274	221.8238
V_{max} (p.u.)	1.0122	1	1	1	1.0121	1.0042	1	1
V_{min} (p.u.)	0.9546	0.9756	0.9431	0.9650	0.9412	0.9588	0.9412	0.9588

TABLE VI
QUALITATIVE COMPARISON OF THE PROPOSED ARTICLE WITH THE EXISTING WORK

Parameter	References				Proposed
	[15]- [17]	[18]	[19]	[20]	
Demand limit	Fixed	Fixed	Not considered	Dynamic	Dynamic
Feed-in limit	Not considered	Not considered	Dynamic	Not considered	Dynamic
Day-to-day management	Not considered	Flexible	Not considered	Not considered	Flexible

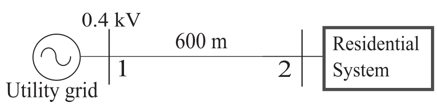

Fig. 13. Residential system connected in the LV distribution network.

and 2.852 kW for Cases 1–4, respectively. This indicates that the peak utility grid demand is less for the proposed method as compared to [18] in all cases. It means an improved PPS is achieved with the proposed method. This is because, in the proposed method, the demand limit is determined optimally by minimizing the peak energy drawn from the utility grid. Moreover, the possibility of limiting the peak utility grid demand to an optimal value is presented in this article considering various cases, i.e., Cases 1–4.

2) Energy Cost: The energy cost of the system over a day is analyzed. For this, the time-of-use price of the energy is considered [25]. The peak time is when load demand is more than 75% of the peak load with an energy price of 5.39 INR. The off-peak time is when load demand is less than 25% of the peak load with an energy price of 4.15 INR. The energy price for the remaining time is 4.39 INR [26]. The EC is calculated as

$$EC = \sum_{t=1}^{T} E_{\text{grid}-d}(t) \times EP(t). \tag{33}$$

$E_{\text{grid}-d}(t) = E_{\text{grid}}$ if $E_{\text{grid}} > 0$ and $E_{\text{grid}-d}(t) = 0$ if $E_{\text{grid}} \leq 0$.

3) Voltage Profile: To show the impact of the proposed peak shaving control on the voltage profile, a two-bus system, as shown in Fig. 13, is considered. The system represents the considered residential system connected in a low-voltage (LV) distribution network. Buses 1 and 2 are considered as slack bus and load bus, respectively. The resistance and reactance of line are 3.69 and 0.094 Ω/km, respectively [27]. The voltage of the load bus over a day is determined using the backward–forward sweep power flow method [28].

The obtained EC, $V_{\max}$, and $V_{\min}$ values for four cases are shown in Table V. The ECs without BESS for Cases 1–4 are 162.3459, 217.2627, 179.2068, and 228.1274 INR/day, respectively. The ECs with the BESS using the proposed control for Cases 1 to 4 are 149.5737, 209.7624, 166.5379, and 221.8238 INR/day, respectively. This indicates that the energy costs are less with the proposed method as compared to the case without the BESS.

$V_{\max}$ without BESS for Cases 1–4 are 1.0122, 1, 1.0122, and 1 p.u., respectively. $V_{\max}$ with the BESS using the proposed control for Cases 1–4 are 1, 1, 1.0042, and 1 p.u., respectively. The $V_{\max}$ values are less with the proposed method as compared to the case without BESS. $V_{\min}$ without BESS for Case 1 to 4 are 0.9546 p.u., 0.9431 p.u., 0.9412 p.u., and 0.9412 p.u., respectively. $V_{\min}$ with BESS using the proposed control for Cases 1–4 are 0.9756, 0.965, 0.9588, and 0.9588 p.u., respectively. The $V_{\min}$ values are more with the proposed method as compared to the case without BESS. This shows that both voltage drop and voltage rise are limited with the consideration of both demand and feed-in limits in the proposed peak shaving control method.

4) Qualitative Comparison: The qualitative comparison of the proposed article with the existing work is shown in Table VI. This indicates that in the existing literature, both demand and feed-in limits together are not considered. However, in the proposed method, both demand and feed-in limits are considered while maintaining the flexible day-to-day management of the system. Moreover, demand and feed-in limits are considered dynamic. It means the demand and feed-in limits vary as per the available predictions of PV power and load demand of the day.

VIII. CONCLUSION

In this article, a general method of determination of optimal dynamic demand and feed-in limits is developed for a grid-connected PV source with a battery. An optimal rule-based peak shaving control algorithm is proposed to limit utility grid power at computed demand and feed-in limits. The proposed control algorithm is tested for various possible cases of demand and PV power profiles. The obtained results show that the utility grid demand and feed-in powers are limited to respective demand and feed-in limits of the day, respectively, for all cases. Moreover, the SoC at the end of the day is maintained equal to the SoC at the start of the day for flexible day-to-day management. The comparison of the proposed control algorithm with the existing work is shown qualitatively and quantitatively. This indicates that the proposed control algorithm provides improved percentage peak shaving as compared to the existing work. Moreover, the reduction of the energy cost of the system and improved voltage profile with the proposed control algorithm is presented.

REFERENCES

[1] C. Kumar, R. Zhu, G. Buticchi, and M. Liserre, “Sizing and SOC management of a smart-transformer-based energy storage system,” *IEEE Trans. Ind. Electron.*, vol. 65, no. 8, pp. 6709–6718, Aug. 2018.

[2] H. Alharbi and K. Bhattacharya, “Stochastic optimal planning of battery energy storage systems for isolated microgrids,” *IEEE Trans. Sustain. Energy*, vol. 9, no. 1, pp. 211–227, Jan. 2018.

[3] J. von Appen and M. Braun, “Sizing and improved grid integration of residential PV systems with heat pumps and battery storage systems,” *IEEE Trans. Energy Convers.*, vol. 34, no. 1, pp. 562–571, Mar. 2019.

[4] X. Yan, C. Gu, X. Zhang, and F. Li, “Robust optimization-based energy storage operation for system congestion management,” *IEEE Syst. J.*, vol. 14, no. 2, pp. 2694–2702, Jun. 2020.

[5] S. L. Arun and M. P. Selvan, “Intelligent residential energy management system for dynamic demand response in smart buildings,” *IEEE Syst. J.*, vol. 12, no. 2, pp. 1329–1340, Jun. 2018.

[6] K. A. Joshi, N. M. Pindoriya, and A. K. Srivastava, “A two-stage fuzzy multiobjective optimization for phase-sensitive day-ahead dispatch of battery energy storage system,” *IEEE Syst. J.*, vol. 12, no. 4, pp. 3649–3660, Dec. 2018.

[7] M. Fekri Moghadam, M. Metcalfe, W. G. Dunford, and E. Vaahedi, “Demand side storage to increase hydroelectric generation efficiency,” *IEEE Trans. Sustain. Energy*, vol. 6, no. 2, pp. 313–324, Apr. 2015.

[8] M. G. Damavandi, J. R. Martí, and V. Krishnamurthy, “A methodology for optimal distributed storage planning in smart distribution grids,” *IEEE Trans. Sustain. Energy*, vol. 9, no. 2, pp. 729–740, Apr. 2018.

[9] K. R. Reddy and S. Meikandasivam, “Load flattening and voltage regulation using plug-in electric vehicle’s storage capacity with vehicle prioritization using ANFIS,” *IEEE Trans. Sustain. Energy*, vol. 11, no. 1, pp. 260–270, Jan. 2020.

[10] A. K. Barnes, J. C. Balda, and A. Escobar-Mejía, “A semi-Markov model for control of energy storage in utility grids and microgrids with PV generation,” *IEEE Trans. Sustain. Energy*, vol. 6, no. 2, pp. 546–556, Apr. 2015.

[11] F. Hafiz, M. A. Awal, A. R. de Queiroz, and I. Husain, “Real-time stochastic optimization of energy storage management using deep learning-based forecasts for residential PV applications,” *IEEE Trans. Ind. Appl.*, vol. 56, no. 3, pp. 2216–2226, May/Jun. 2020.

[12] L. Lengyel, “Validating rule-based algorithms,” *J. Appl. Sci.*, vol. 12, no. 4, pp. 59–75, 2015.

[13] U. Kumar Jha, N. Soren, and A. Sharma, “An efficient HEMS for demand response considering TOU pricing scheme and incentives,” in *Proc. 2nd Int. Conf. Power, Energy Environ.: Towards Smart Technol.*, 2018, pp. 1-6.

[14] S. Bruno, G. Giannoccaro, and M. La Scala, “A demand response implementation in tertiary buildings through model predictive control,” *IEEE Trans. Ind. Appl.*, vol. 55, no. 6, pp. 7052–7061, Nov./Dec. 2019.

[15] J. Leadbetter and L. Swan, “Battery storage system for residential electricity peak demand shaving,” *Energy Buildings*, vol. 55, pp. 685–692, 2012.

[16] K. Mahmud, M. J. Hossain, and G. E. Town, “Peak-load reduction by coordinated response of photovoltaics, battery storage, and electric vehicles,” *IEEE Access*, vol. 6, pp. 29353–29365, 2018.

[17] D. M. Greenwood, N. S. Wade, P. C. Taylor, P. Papadopoulos, and N. Heyward, “A probabilistic method combining electrical energy storage and real-time thermal ratings to defer network reinforcement,” *IEEE Trans. Sust. Energy*, vol. 8, no. 1, pp. 374–384, Jan. 2017.

[18] Y. Riffonneau, S. Bacha, F. Barruel, and S. Ploix, “Optimal power flow management for grid connected PV systems with batteries,” *IEEE Trans. Sustain. Energy*, vol. 2, no. 3, pp. 309–320, Jul. 2011.

[19] G. Angenendt, S. Zurmühlen, R. Mir-Montazeri, D. Magnor, and D. U. Sauer, “Enhancing battery lifetime in PV battery home storage system using forecast based operating strategies,” *Energy Procedia*, vol. 99, pp. 80–88, 2016.

[20] D. T. Vedullapalli, R. Hadidi, and B. Schroeder, “Combined HVAC and battery scheduling for demand response in a building,” *IEEE Trans. Ind. Appl.*, vol. 55, no. 6, pp. 7008–7014, Nov./Dec. 2019.

[21] K. Gaur, H. Kumar, R. P. K. Agarwal, K. V. S. Baba, and S. K. Soonee, “Analysing the electricity demand pattern,” in *Proc. Nat. Power Syst. Conf.*, Dec. 2016, pp. 1–6.

[22] S. Chun and A. Kwasinski, “Analysis of classical root-finding methods applied to digital maximum power point tracking for sustainable photovoltaic energy generation,” *IEEE Trans. Power Electron.*, vol. 26, no. 12, pp. 3730–3743, Dec. 2011.

[23] M. Hosseinzadeh and F. R. Salmasi, “Robust optimal power management system for a hybrid AC/DC micro-grid,” *IEEE Trans. Sustain. Energy*, vol. 6, no. 3, pp. 675–687, Jul. 2015.

[24] W. K. A. Najy, H. H. Zeineldin, and W. L. Woon, “Optimal protection coordination for microgrids with grid-connected and islanded capability,” *IEEE Trans. Ind. Electron.*, vol. 60, no. 4, pp. 1668–1677, Apr. 2013.

[25] Y. Hong and M. Wu, “Markov model-based energy storage system planning in power systems,” *IEEE Syst. J.*, vol. 13, no. 4, pp. 4313–4323, Dec. 2019.

[26] Economics Division Central Electricity Regulatory Commission, “Short-term power market in India: 2018–19,” Accessed: Jul. 09, 2019. [Online]. Available: http://www.cercind.gov.in/annual report.html

[27] *Benchmark System for Network Integration of Renewable and Distribution Energy Resources*, Technical Brochure, Cigre Task Force C6.04.02, 2014.

[28] S. Ganguly, “Multi-objective planning for reactive power compensation of radial distribution networks with unified power quality conditioner allocation using particle swarm optimization,” *IEEE Trans. Power Syst.*, vol. 29, no. 4, pp. 1801-1810, Jul. 2014.

Rampelli Manojkumar (Student Member, IEEE) received the B.E. degree in electrical and electronics engineering from the Vasavi College of Engineering, Hyderabad, India, in 2013, and the M.Tech. degree in power and energy systems from the National Institute of Technology Karnataka, Surathkal, India, in 2015. He is currently working toward the Ph.D. degree with the Department of Electronics and Electrical Engineering, Indian Institute of Technology Guwahati, Guwahati, India.

His research interests include optimal energy management control in residential distribution systems and smart grids.

Chandan Kumar (Senior Member, IEEE) received the B.Sc. degree from the Muzaffarpur Institute of Technology, Muzaffarpur, India, in 2009, the M.Tech. degree from the National Institute of Technology, Trichy, India, in 2011, and the Ph.D. degree from the Indian Institute of Technology Madras, Chennai, India, in 2014, all in electrical engineering.

Since 2015, he has been an Assistant Professor with the Electronics and Electrical Engineering Department, Indian Institute of Technology Guwahati, Guwahati, India. From 2016 to 2017, he was an Alexander von Humboldt Research Fellow with the Chair of Power Electronics, University of Kiel, Kiel, Germany. His research interests include power electronics application in power systems, power quality, and renewable energy.

Sanjib Ganguly (Senior Member, IEEE) was born in India in 1981. He received the B.E. degree from the Indian Institute of Engineering Science and Technology, Shibpur, India, in 2003, and the M.E. degree from Jadavpur University, Kolkata, India, 2006, both in electrical engineering, and the Ph.D. degree from the Indian Institute of Technology Kharagpur, Kharagpur, India, in 2011.

He is currently an Associate Professor with the Department of Electronics and Electrical Engineering, Indian Institute of Technology Guwahati, Guwahati, India. His research interests include power system operation and planning, custom power devices, hybrid energy systems, and evolutionary algorithms.

João P. S. Catalão (Senior Member, IEEE) received the M.Sc. degree from the Instituto Superior Técnico, Lisbon, Portugal, in 2003, and the Ph.D. and Habilitation degrees from the University of Beira Interior, Covilhã, Portugal, in 2007 and 2013, respectively.

He is currently a Professor with the Faculty of Engineering, University of Porto, Porto, Portugal, where he is also a Research Coordinator with the Institute for Systems and Computer Engineering, Technology, and Science. His research interests include power system operations and planning, distributed renewable generation, demand response, and smart grids.